

Cite this: *Phys. Chem. Chem. Phys.*,
2023, 25, 20042

The increase of europium-based OLED luminance through reducing the excited state lifetime by mixed-ligand complex formation†

 Makarii I. Kozlov,^{id}*^a Andrey A. Vashchenko,^b Alexander A. Pavlov,^{id}^{cd}
 Alexander S. Goloveshkin,^c Egor V. Latipov,^{id}^e Natalia P. Kuzmina^a and
 Valentina V. Utochnikova^{id}*^a

An approach to the luminance increase of the europium-based OLED is proposed through the formation of the mixed-ligand complex. The introduction of two diverse anionic ligands around one europium ion forming a mixed-ligand complex is confirmed by powder X-ray diffraction, ¹H and ¹⁹F NMR spectroscopy, MALDI MS spectroscopy, and luminescence spectroscopy. A decrease in the symmetry of the coordination environment leads to a 50% reduction of the lifetime of the excited state. The obtained OLEDs based on mixed ligand europium complexes are significantly superior in luminance to OLEDs based on individual complexes.

Received 7th May 2023,
Accepted 3rd July 2023

DOI: 10.1039/d3cp02082g

rsc.li/pccp

Introduction

Organic light-emitting diodes (OLEDs) are among the market leaders in devices used for portable electronics and displays in smartphones, TVs, and laptops.¹ Despite the widespread use of OLEDs, the world scientific community still faces some major challenges. One such challenge is improving the color purity,² which is attempted by the development of new compounds^{3,4} and also by various technological methods, such as filters that reduce the spectral bandwidth.⁵

The highest color purity can be achieved by using the lanthanide coordination compounds (CCs), which are well-known for their narrow luminescence bands due to their unique f-f transitions.^{6–8} However, lanthanide-based OLEDs still demonstrate significantly lower efficiencies compared to phosphorescent iridium compounds^{9–11} and rapidly developing TADF-based materials.^{12–14} Thus, the search for promising

ways to improve the efficiency of lanthanide-based OLEDs is becoming an important task.

Recently, it was clarified by our group that the key factor hampering the electroluminescence (EL) efficiency of lanthanide-based organic light emitting diodes (OLEDs) is the long observed lifetime of the excited state of lanthanide coordination compounds.¹⁵ Therefore, various approaches are proposed in order to reduce the lifetime. The observed lifetime (τ_{obs}) is equal to

$$\tau_{\text{obs}} = \frac{1}{k_{\text{rad}} + \sum k_{\text{nr}}}$$

where k_{rad} is the radiative relaxation constant, and k_{nr} is a non-radiative process constant.¹⁶ Aiming at the increase of the k_{nr} , the introduction of the quenching ligand has already demonstrated its effectiveness in OLED performance increase^{17–21} even despite the simultaneous decrease of the quantum yield (PLQY). In the present paper, we aim at the increase of the k_{rad} and develop a novel approach toward shortening the observed lifetime.

The lanthanide luminescence corresponds to the Laporte-forbidden f-f transitions,^{16,22,23} and therefore the radiative relaxation constant directly depends on the symmetry of the coordination environment of the lanthanide ion: the lower the symmetry, the more allowed f-f transitions become, and, consequently, the more k_{rad} increases. To reduce the symmetry of the coordination environment, we proposed to introduce various ligands around one lanthanide ion. The approach of symmetry reduction of the Eu³⁺ coordination environment by the development of an anionic ligand was proposed earlier by

^a M. V. Lomonosov Moscow State University, 1/3 Leninskiye Gory, Moscow, 119991, Russia. E-mail: valentina.utochnikova@gmail.com

^b P. N. Lebedev Physical Institute, Leninsky prosp. 53, Moscow, 119992, Russia

^c A. N. Nesmeyanov Institute of Organoelement Compounds, Vavilova St. 28, Moscow, 119334, Russia

^d BMSTU Center of National Technological Initiative "Digital Material Science: New Material and Substances", Bauman Moscow State Technical University, 2nd Baumanskaya st. 5, Moscow, Russia

^e Institute of Nanotechnology of Microelectronics of the Russian Academy of Sciences, Leninsky Prospect 32A, Moscow, 119334, Russia

† Electronic supplementary information (ESI) available: Synthesis and experimental methods, PXRD, TGA, IR- and NMR- spectroscopy data. See DOI: <https://doi.org/10.1039/d3cp02082g>

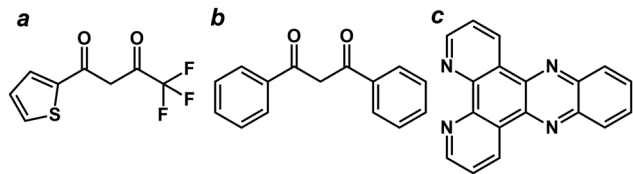


Fig. 1 Ligands used in the present study: (a) Htta, (b) Hdbm, and (c) DPPZ.

L. Zhang *et al.*^{20,24} and led to the highest obtained luminance of the Eu-based OLEDs so far. Moreover, the approach of increasing the diversity of ligands coordinated to the lanthanide ion was studied by N. Lima *et al.*^{25,26} Using two different neutral ligands allowed the increase of the radiative rate constants, which also resulted in up to twice the quantum yield increase. At the same time, this approach was only applied to improve the photoluminescence efficiency and was never proposed to increase the efficiency of the lanthanide-based OLEDs. This is the goal of the present paper.

In order to check the proposed approach, we selected europium β -diketonates, since they are well-known for their record luminance and efficiencies among lanthanide-based OLED emitters.^{27,28} In particular, dibenzoylmethane (Hdbm) and thionyltrifluoroacetone (Htta) were chosen as anionic ligands (Fig. 1), since they are known for effective sensitization of the europium ion.^{29,30} Besides, some of the brightest europium-based OLEDs were obtained with the use of europium complexes with these ligands.^{20,31,32} Moreover, dipyrido[3,2-*a*:2'-*c*,3'-*c'*]phenazine (DPPZ) (Fig. 1) is known as a ligand with low triplet energy, which causes efficient back energy transfer and results in reduction of the observed lifetime.¹⁷

To obtain mixed-ligand complexes (MLCs), two methods were proposed. One of them consists in the mixing of the individual $\text{Eu}(\text{dbm})_3\text{DPPZ}$ and $\text{Eu}(\text{tta})_3\text{DPPZ}$ complexes in solution, followed by the resulting solution evaporation to dryness. Whereas by another one, a mixed-ligand complex is synthesized using the homogeneous mixture of two anionic ligands in solution, and the obtained product is assigned as $\text{Eu}(\text{dbm} + \text{tta})_3\text{DPPZ}$.

Thus, as the objects of our research, individual complexes $\text{Eu}(\text{dbm})_3\text{DPPZ}$ and $\text{Eu}(\text{tta})_3\text{DPPZ}$, as well as mixed-ligand complexes $\text{Eu}(\text{dbm} + \text{tta})_3\text{DPPZ}$ and $[\text{Eu}(\text{dbm})_3\text{DPPZ} + \text{Eu}(\text{tta})_3\text{DPPZ}]$, obtained by different methods, were selected. The determination of whether mixed ligand complexes, and not the mixture of individual complexes, were obtained, is in the scope of the present work, as well as the comparison of these two complexes and, finally, the study of the influence of the proposed approach on the OLED luminance.

Experimental section

Synthesis

All the reagents and the solvents were purchased from commercial sources.

Synthesis of $\text{Eu}(\text{L})_3\text{DPPZ}$ (L = dbm or tta). A solution of 1 mmol of $\text{EuCl}_3 \cdot 6\text{H}_2\text{O}$ in 20 ml of ethanol was added to a

mixture of HL (3 mmol) and Et_3N (3 mmol) in 20 ml of ethanol, then a solution of DPPZ (1 mmol) in 30 ml of ethanol was added, and the precipitation was observed. The reaction mixture was stirred for 2 h, and then the precipitate was filtered off, washed with cold ethanol, and dried in air.

Synthesis of $\text{Eu}(\text{dbm} + \text{tta})_3\text{DPPZ}$. A solution of 1 mmol of $\text{EuCl}_3 \cdot 6\text{H}_2\text{O}$ in 20 ml of ethanol was added to a mixture of Htta (1.5 mmol), Hdbm (1.5 mmol), and Et_3N (3 mmol) in 20 ml of ethanol, then a solution of DPPZ (1 mmol) in 30 ml of ethanol was added, and the precipitation was observed. The reaction mixture was stirred for 2 h, and then the precipitate was filtered off, washed with cold ethanol, and dried in air.

Synthesis of $\text{Eu}(\text{dbm})_3\text{DPPZ} + \text{Eu}(\text{tta})_3\text{DPPZ}$. Two obtained individual complexes $\text{Eu}(\text{dbm})_3\text{DPPZ}$ and $\text{Eu}(\text{tta})_3\text{DPPZ}$ were dissolved in THF, then two equimolar solutions of the complexes were mixed, followed by the resulting solution evaporation to dryness.

Methods

X-ray powder diffraction (XRD) patterns were measured on a Bruker D8 Advance diffractometer with a LynxEye detector and Ni filter monochromator, $\lambda(\text{CuK}\alpha) = 1.5416 \text{ \AA}$, θ/θ scan from 5° to 50° , step size 0.020° . The measurements were performed in reflection mode, and the compounds were deposited on a silicon zero-background holder. The refinement of the powder patterns was performed in TOPAS 5.0 software.

^1H NMR spectra and ^{19}F NMR spectra were recorded from the DMSO-d_6 and THF-d_8 solutions with a Bruker Avance 600 NMR spectrometer.

Thermal analysis was carried out on a thermoanalyzer STA 409 PC Luxx (NETZSCH, Germany) in the temperature range of $20\text{--}1000^\circ\text{C}$ in air and at a heating rate of 10°min^{-1} . The evolved gases were simultaneously monitored during the TA experiment using a coupled QMS 403C Aeolus quadrupole mass spectrometer (NETZSCH, Germany). The mass spectra were registered for the species with the following m/z values: 18 (corresponding to H_2O), 44 (corresponding to CO_2) and 46 (corresponding to $\text{C}_2\text{H}_5\text{OH}$).

IR spectra in the ATR mode were recorded on an FTIR Nicolet iS50 spectrometer in the region of $500\text{--}4000 \text{ cm}^{-1}$.

MALDI mass spectra were recorded on a Bruker Autoflex II instrument (resolution FWHM 18000) equipped with a nitrogen laser with an operating wavelength of 337 nm and a time-of-flight mass analyzer operating in reflectron mode. Accelerating voltage 20 kV. The samples were applied to a polished steel substrate. The recording was performed in the mode of positive spectra. The resulting spectrum was the sum of 50 spectra obtained at different points in the sample. The matrices used were 2,5-dihydroxybenzoic acid (DHB) (Acros, 99%) and *a*-cyano-4-hydroxycinnamic acid (HCCA) (Acros, 99%).

Photoluminescence spectra were recorded using a Fluoromax Plus (HORIBA) spectrometer at room temperature; excitation was performed through a ligand, and the absolute method in the integration sphere was used.

OLED fabrication

Glass substrates coated with 15 Ohm sq^{-1} of prepatterned indium tin oxide (Kaivo LTD) were used as anodes. The substrates were cleaned by three-step ultrasonication in deionized water, acetone, and isopropanol for 15 min each followed by drying with airflow. Then, a 20 min UV treatment was performed to remove residual organic impurities.

Hole injection layer PEDOT-PSS (poly(3,4-ethylenedioxythiophene):poly(styrenesulfonate)) (Ossila Al-4083) was spin-coated on cleaned ITO glass substrates at 3000 rpm for 1 min with a subsequent annealing process at 140 °C for 10 min in the air. Then, a 20 nm thick hole-transporting poly-TPD (Ossila) solution was spin-coated from 5 mg mL^{-1} solution in chlorobenzene at 1500 rpm for 1 min and dried at 120 °C for 10 min in a nitrogen-filled glovebox. Afterward, a 30 nm thick emission layer was spin-coated from THF (complex: CBP 1:3, total $c = 5 \text{ g L}^{-1}$) at 1500 rpm for 1 min with further annealing at 80 °C for 10 min.

Finally, the substrates were transferred into a MB-ProVap 5G vacuum deposition system. The ~ 20 nm thick electron-transporting/hole-blocking layer TPBi (Lumtec) was thermally evaporated followed by a ~ 1 nm thick LiF layer and 100 nm thick aluminum layer as the cathode in a sequence through a shadow mask at 10^{-6} mbar to form 21 mm^2 pixels. The thicknesses of all evaporated layers were controlled by a quartz micro-balance resonator pregraduated by profilometry.

Measurements of the OLED characteristics were performed in the N_2 glovebox without encapsulation. The electroluminescence spectra were obtained with an Instrument Systems CAS 120 Array spectrometer sensitive within 200–1100 nm. Current-voltage characteristics were measured by using a Keithley 2400 source-meter measurement unit. The turn-on voltage was defined as the voltage at which 1 cd m^{-2} EL intensity was achieved.

Results and discussion

Synthesis and characterization

Complexes $\text{Eu}(\text{L})_3\text{DPPZ}$ ($\text{L} = \text{tta}$ and dbm) were synthesized from the ethanol solutions of HL (HL = Hdbm or Htta),

europium chloride hexahydrate $\text{EuCl}_3 \cdot 6\text{H}_2\text{O}$, and dipyrindo [3,2-*a*:2'*c*,3'*cc*]phenazine (DPPZ) as in the original papers.^{32–34} Their composition, as well as that of MLCs, was confirmed using thermal analysis (Fig. S2a in ESI[†]), IR-spectroscopy (Fig. S2b, ESI[†]), and ^1H NMR spectroscopy (Fig. 2 and Fig. S3, ESI[†]). The $\text{Eu}(\text{dbm})_3\text{DPPZ}$ powder diffraction pattern was successfully indexed (Fig. S1a, ESI[†]), and the powder diffraction pattern of $\text{Eu}(\text{tta})_3\text{DPPZ}$ was successfully refined by the Rietveld method (Fig. S1b, ESI[†]) using the structure we obtained earlier.¹⁷

To study the possibility of the formation of the mixed-ligand complex, two approaches were used (Scheme 1). The first one consists in the dissolution of the equimolar mixture of two anionic ligands tta^- and dbm^- in ethanol, followed by the synthesis of a mixed-ligand complex $\text{Eu}(\text{dbm} + \text{tta})_3\text{DPPZ}$ using this mixture as a source of anionic ligand. While the second one represents the simple co-dissolution of individual complexes $\text{Eu}(\text{dbm})_3\text{DPPZ}$ and $\text{Eu}(\text{tta})_3\text{DPPZ}$ in THF, followed by the clear solution rotary evaporation to dryness. THF was selected as a solvent suitable for thin film deposition, as we aim for OLED application, where thin films are necessary.

The second method was supposed to be effective due to lanthanide complexes, in particular β -diketonates, being very labile,³⁵ and thus, partial dissociation and ligand exchange is expected during the co-dissolution. This may also result in obtaining the same product by both methods.

The initial task was to determine whether the obtained compounds did indeed represent mixed-ligand complexes, and not a mixture of the individual complexes, as well as to compare them to each other. After that, it was also important to find out if the individual mixed-ligand compound was formed,



Scheme 1 Two approaches to the formation of the mixed-ligand complex.

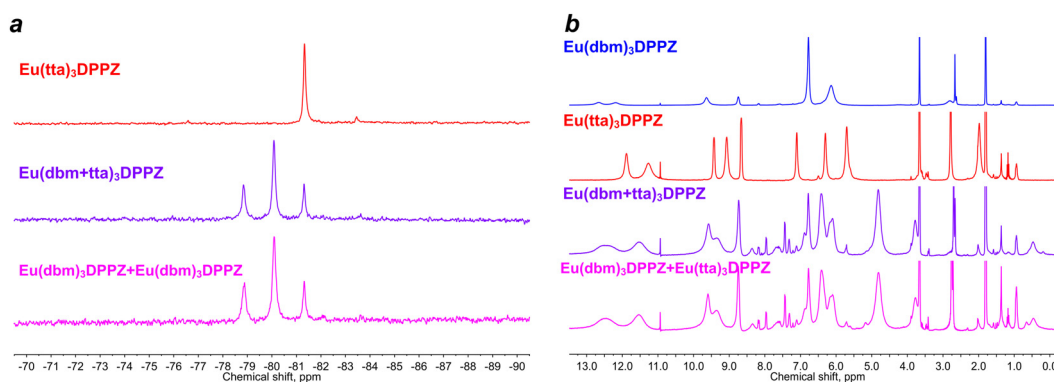


Fig. 2 (a) ^{19}F NMR and (b) ^1H NMR spectra of individual complexes ($\text{Eu}(\text{dbm})_3\text{DPPZ}$ and $\text{Eu}(\text{tta})_3\text{DPPZ}$) and mixed-ligand complexes $\text{Eu}(\text{dbm} + \text{tta})_3\text{DPPZ}$ and $[\text{Eu}(\text{dbm})_3\text{DPPZ} + \text{Eu}(\text{tta})_3\text{DPPZ}]$ (THF-d_8).

or the product represents a statistical mixture, containing all the possible complexes $[\text{Eu}(\text{dbm})_3\text{DPPZ} + \text{Eu}(\text{dbm})_2(\text{tta})\text{DPPZ} + \text{Eu}(\text{tta})_2(\text{dbm})\text{DPPZ} + \text{Eu}(\text{tta})_3\text{DPPZ}]$.

Therefore, a combination of methods of powder X-ray diffraction, ^1H and ^{19}F NMR spectroscopy in THF-d_8 , MALDI MS spectroscopy, and luminescent spectroscopy was used. Direct proof of the mixed-ligand individual complex formation is very complicated, and therefore, although ^1H and ^{19}F NMR spectroscopy can only determine the complex composition and structure in solution, it is very informative as it sheds light on the processes preceding the complex formation. Thus, THF-d_8 was selected as a solvent for the NMR study, due to OLED thin films being deposited from THF.

Because of the presence of the unpaired electrons in lanthanide ions, the signals in the NMR spectra of their complexes can be shifted and broadened in comparison to the complexes with diamagnetic ions.³⁶ This shift depends on the distance from the analyzed nucleus to the lanthanide ion, as well as on the total complex geometry. It makes the spectra very sensitive to the slightest changes in the coordination environment, including ligand exchange.

The comparison of the obtained spectra with each other revealed that in the ^{19}F spectrum of $\text{Eu}(\text{tta})_3\text{DPPZ}$, the only signal is expectedly observed, whereas $\text{Eu}(\text{dbm})_3\text{DPPZ}$ contains no fluorine atoms at all. While both spectra of the $\text{Eu}(\text{dbm} + \text{tta})_3\text{DPPZ}$ complex and a mixture of individual complexes $[\text{Eu}(\text{dbm})_3\text{DPPZ} + \text{Eu}(\text{tta})_3\text{DPPZ}]$ contain three signals, indicating that they dissociate into three different forms in THF-d_8 (Fig. 2(a)). This corresponds to the entry of 1, 2, and 3 anionic ligands into the coordination sphere of each europium ion. The coincidence of the ^{19}F NMR spectra of the $[\text{Eu}(\text{dbm})_3\text{DPPZ} + \text{Eu}(\text{tta})_3\text{DPPZ}]$ and $\text{Eu}(\text{dbm} + \text{tta})_3\text{DPPZ}$ complexes confirms the identical composition of both products.

This is clearly seen in the case of the ^1H NMR spectra (Fig. 2(b)) of $[\text{Eu}(\text{dbm})_3\text{DPPZ} + \text{Eu}(\text{tta})_3\text{DPPZ}]$ and $\text{Eu}(\text{dbm} + \text{tta})_3\text{DPPZ}$ complexes, for which the proton signals absolutely coincide. The presence of new signals in the mixed-ligand complex spectra, rather than only the summation of the signals

of individual compounds, indicates the mixed-ligand complex formation. In the case of paramagnetic compounds, the slightest structural changes in the solution lead to significant changes in the magnetic properties and, consequently, to significant paramagnetic shifts.³⁶ Therefore, the same paramagnetic shifts in both the ^{19}F and ^1H spectra of the obtained mixed-ligand complexes mean the structural identity of the obtained compounds.

In order to study the ratio of anionic ligands in mixed-ligand complexes $\text{Eu}(\text{dbm} + \text{tta})_3\text{DPPZ}$ and $[\text{Eu}(\text{dbm})_3\text{DPPZ} + \text{Eu}(\text{tta})_3\text{DPPZ}]$, MALDI spectroscopy was carried out. During the ionization of the investigated substances, the elimination of one anionic ligand occurs for both individual complexes and mixed-ligand complexes. In MALDI MS spectra of individual complexes $\text{Eu}(\text{dbm})_3\text{DPPZ}$ and $\text{Eu}(\text{tta})_3\text{DPPZ}$, only signals corresponding to the theoretical isotopic distribution of $\text{Eu}(\text{L})_2\text{DPPZ}^+$ are present (Fig. 3(a)). In the case of mixed-ligand complexes $\text{Eu}(\text{dbm} + \text{tta})_3\text{DPPZ}$ and $[\text{Eu}(\text{dbm})_3\text{DPPZ} + \text{Eu}(\text{tta})_3\text{DPPZ}]$, the most intense signals correspond to the $\text{Eu}(\text{dbm})(\text{tta})\text{DPPZ}^+$ complex. However, the presence of signals of both $\text{Eu}(\text{dbm})_2\text{DPPZ}^+$ and $\text{Eu}(\text{tta})_2\text{DPPZ}^+$ speaks in favour of statistical distribution of anionic ligands dbm^- and tta^- in mixed-ligand complexes.

The powder X-ray diffraction (PXRD) analysis also confirmed the absence of individual complexes in each of the products. Both $\text{Eu}(\text{dbm})_3\text{DPPZ}$ and $\text{Eu}(\text{tta})_3\text{DPPZ}$ represent highly crystalline solids, while the PXRD patterns of $\text{Eu}(\text{dbm} + \text{tta})_3\text{DPPZ}$ and $[\text{Eu}(\text{dbm})_3\text{DPPZ} + \text{Eu}(\text{tta})_3\text{DPPZ}]$ correspond to an amorphous substance, not containing the reflexes corresponding to the individual complexes (Fig. 3(b)). Furthermore, the amorphous nature of these patterns speaks in favour of the formation of the individual complex $\text{Eu}(\text{dbm} + \text{tta})_3\text{DPPZ}$, where dbm^- and tta^- ligands statistically occupy the positions around the central europium ions. This is further confirmed by the luminescence data, discussed in the corresponding section.

Thus, we can conclude that both obtained compounds are mixed-ligand, they have the same composition and they do not contain the individual complexes even as mixture components.

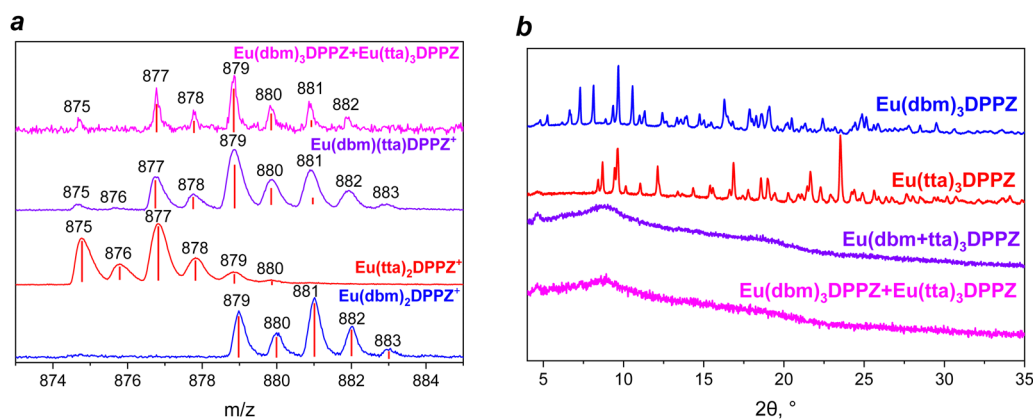


Fig. 3 (a) MALDI spectra of individual complexes ($\text{Eu}(\text{dbm})_3\text{DPPZ}$ and $\text{Eu}(\text{tta})_3\text{DPPZ}$) and mixed-ligand complexes $\text{Eu}(\text{dbm} + \text{tta})_3\text{DPPZ}$ and $[\text{Eu}(\text{dbm})_3\text{DPPZ} + \text{Eu}(\text{tta})_3\text{DPPZ}]$; the theoretical isotope distribution is indicated by red sticks. (b) PXRD patterns (normalized) of individual complexes ($\text{Eu}(\text{dbm})_3\text{DPPZ}$ and $\text{Eu}(\text{tta})_3\text{DPPZ}$) and mixed-ligand complexes $\text{Eu}(\text{dbm} + \text{tta})_3\text{DPPZ}$ and $[\text{Eu}(\text{dbm})_3\text{DPPZ} + \text{Eu}(\text{tta})_3\text{DPPZ}]$.

Moreover, they rather correspond to the individual complex $\text{Eu}(\text{dbm} + \text{tta})_3\text{DPPZ}$, where dbm^- and tta^- are statistically localized around the Eu^{3+} ion.

Photoluminescence properties

All photoluminescence properties were studied for the thin films, as complexes are used in OLEDs in the thin film state. Thin films of individual complexes ($\text{Eu}(\text{dbm})_3\text{DPPZ}$ and $\text{Eu}(\text{tta})_3\text{DPPZ}$) and mixed-ligand complexes ($\text{Eu}(\text{dbm} + \text{tta})_3\text{DPPZ}$ and $[\text{Eu}(\text{dbm})_3\text{DPPZ} + \text{Eu}(\text{tta})_3\text{DPPZ}]$), as well as composite films, where the complexes were doped into ambipolar host CBP (4,4'-bis(9-carbazolyl)-2,2'-biphenyl) (75% wt% of CBP), then were spin-coated onto quartz glass from THF solution (5 g L^{-1}) at 1500 rpm, and further annealed at 80°C for 20 min, similarly as further during OLED fabrication.

We measured absorption spectra, excitation spectra, luminescence spectra, photoluminescence quantum yields, and observed lifetimes. These data were obtained under the same conditions in the same experiment for films deposited under the same conditions. Therefore, we suggested that it is possible to present these values with higher accuracy than that of the PLQY determination method (above 1%).

The photoluminescence (PL) spectra of individual and mixed-ligand complexes (both pure and doped into CBP), coincide with each other and correspond to the luminescence of Eu^{3+} (Fig. 4(b) and (d)). However, the luminescence of undoped films was much less intense, and the luminescence of the DPPZ ligand was observed for undoped films.

The photoluminescent excitation (PLE) spectra of the undoped films correspond to the absorption of dbm^- , tta^- , and DPPZ ligands and possess quite close maximum positions (Fig. 4(a)). In the case of films, doped into CBP, the form of the excitation spectra is changed, witnessing the additional through-CBP excitation of Eu^{3+} luminescence (Fig. 4(c)). Expectedly, no noticeable change in the shape of the excitation bands is observed after the formation of both $\text{Eu}(\text{dbm} + \text{tta})_3\text{DPPZ}$ and $[\text{Eu}(\text{dbm})_3\text{DPPZ} + \text{Eu}(\text{tta})_3\text{DPPZ}]$.

The PLQY values of the obtained films were equal among both doped and undoped films (Table 1). This is unexpected, since in previous work²⁵ the increase of the PLQY was observed due to the mixed-ligand complex formation. It can be explained by the presence of the efficient quencher DPPZ ligand, which levels off the positive impact of the lifetime decrease. This PLQY equality, however, is useful for the current research, as it allows the further direct comparison of the OLED performance.

Unlike PL and PLE spectra, as well as PLQY values, the observed lifetimes underwent a significant change upon MLC formation. The lifetimes of individual complexes $\text{Eu}(\text{dbm})_3\text{DPPZ}$ and $\text{Eu}(\text{tta})_3\text{DPPZ}$ (79 μs and 110 μs , respectively) are rather low compared to typical coordination compounds of europium, which is associated with luminescence quenching by the DPPZ ligand,¹⁷ as well as with the easy polarizability of β -diketonates.¹⁵ However, the observed lifetimes of the mixed-ligand complexes $\text{Eu}(\text{dbm} + \text{tta})_3\text{DPPZ}$ and $[\text{Eu}(\text{dbm})_3\text{DPPZ} + \text{Eu}(\text{tta})_3\text{DPPZ}]$ (65 μs and 67 μs , Table 1) were even lower than that of individual complexes and, moreover,

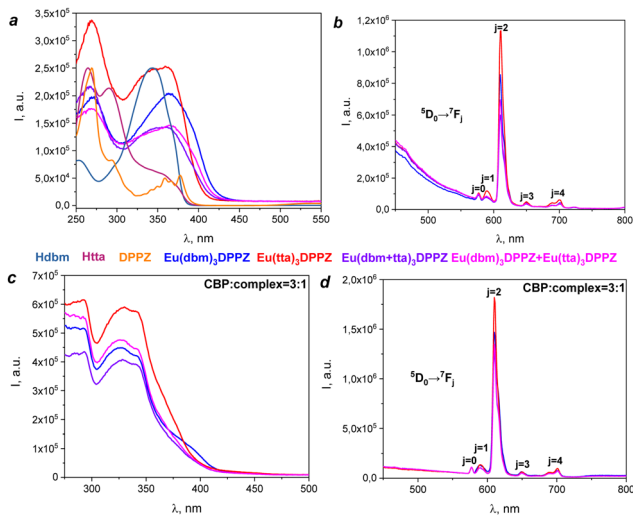


Fig. 4 (a) Excitation ($\lambda_{\text{em}} = 612 \text{ nm}$) of pure europium complex films and absorption spectra of the ligands, and (b) luminescence spectra ($\lambda_{\text{ex}} = 360 \text{ nm}$) of pure europium complex films. (c) Excitation ($\lambda_{\text{em}} = 612 \text{ nm}$) and (d) luminescence spectra ($\lambda_{\text{ex}} = 330 \text{ nm}$) of composite films (CBP : complex = 3 : 1).

Table 1 Photoluminescence and transport properties of the obtained films of europium complexes

Complex	PLQY, %	τ_{obs} , μs	CBP films PLQY, %	CBP films τ_{obs} , ms
$\text{Eu}(\text{dbm})_3\text{DPPZ}$	4.8	79	3.2	0.32
$\text{Eu}(\text{tta})_3\text{DPPZ}$	5.3	110	4.6	0.36
$\text{Eu}(\text{dbm} + \text{tta})_3\text{DPPZ}$	5.0	65	4.2	0.28
$[\text{Eu}(\text{dbm})_3\text{DPPZ} + \text{Eu}(\text{tta})_3\text{DPPZ}]$	5.2	67	3.5	0.27

equal to each other (Fig. 5(a)). This confirms the hypothesis put forward that by reducing the symmetry of the coordination environment, it is possible to achieve a decrease in the lifetime of the excited state, and additionally speaks in favour of the same structure of both mixed-ligand complexes. For the doped films, this difference is less pronounced; however, both MLCs also demonstrate equal lifetimes, which are lower than those of both initial complexes.

It is especially important that all the measured decay curves, including those of MLCs, were monoexponential (Error! Reference source not found.), which confirms the formation of individual complexes. Thus, the obtained mixed-ligand complexes can be considered as the individual complex $\text{Eu}(\text{dbm} + \text{tta})_3\text{DPPZ}$, where dbm^- and tta^- are statistically localized around the Eu^{3+} ion.

Electroluminescence properties

In order to study the effect of the observed lifetime on the electroluminescence efficiency, the obtained thin films were tested as emission layers in OLEDs. OLEDs were manufactured with the same heterostructure (Table 2), which had already

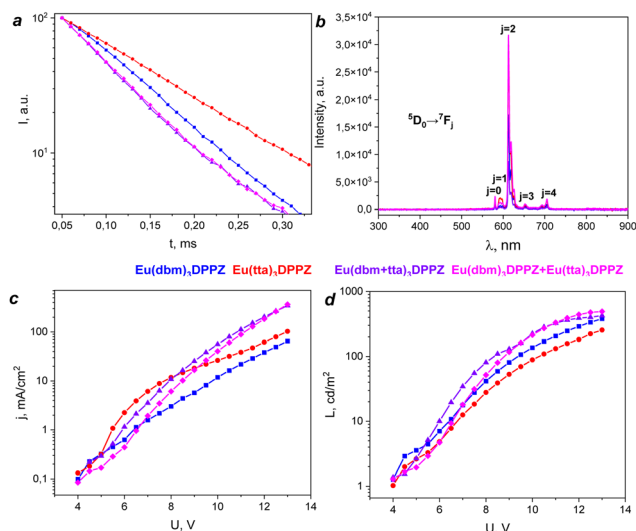


Fig. 5 (a) Normalized decay curves ($\lambda_{\text{ex}} = 360$ nm, $\lambda_{\text{em}} = 612$ nm) of pure europium complex films; (b) electroluminescence spectra of OLEDs 1–4 at the U_{on} voltage; (c) I – V curves of OLEDs 1–4; (d) L – V curves of OLEDs 1–4.

been tested for europium coordination compounds:³⁷ ITO/PEDOT:PSS/poly-TPD/CBP:emitter (3 : 1 wt%)/TPBi/LiF/Al.

We selected CBP as a host material in EML due to: (1) its high HOMO level (5.9 eV) and high excited state energy (2.6 eV), suitable to cause efficient energy transfer to europium luminescence,³⁸ (2) it is an ambipolar host,³⁹ and (3) it is known as the best host for solution-processed OLEDs.⁴⁰ The doping concentration (25 wt%) was selected based on our previous study.¹⁷

All the obtained OLEDs demonstrated solely typical intense electroluminescence spectra of europium ions (Fig. 5(b)). According to their I – V curves, a high current density is observed, associated with the expected good transport properties of the obtained compounds (Fig. 5(b)).

The maximum luminance of the OLEDs 1 and 2, based on the individual $\text{Eu}(\text{dbm})_3\text{DPPZ}$ and $\text{Eu}(\text{tta})_3\text{DPPZ}$ complexes, reached 381 cd m^{-2} and 255 cd m^{-2} at 13 V (Fig. 5(d)), respectively. It is important to note that both complexes demonstrate the same PLQY. Despite this fact, OLED 1 demonstrates clearly higher luminance in the whole bias range, which can only be explained by its remarkably lower observed lifetime (Table 1).

As expected, both MLCs demonstrated EL luminance, exceeding those of individual complexes, up to 502 cd m^{-2} for $[\text{Eu}(\text{dbm})_3\text{DPPZ} + \text{Eu}(\text{tta})_3\text{DPPZ}]$ at 13 V. Both OLED 3 and OLED 4 demonstrated the same luminance up to 11 V, though

above this value a slight difference was observed, probably, due to the different current density at a higher voltage.

An obtained 25% increase in luminance cannot be explained by anything other than the lifetime change. In fact, the PLQYs of both complexes and doped films are equal, and the charge carrier mobilities for MLC are of the same order as for individual complexes. Thus, mixed ligand complex formation leads to a 25% increase in luminance in comparison to those based on individual complexes due to the decrease in the lifetime of the excited state.

Conclusions

Two approaches resulted in the formation of the same mixed-ligand complex $\text{Eu}(\text{dbm} + \text{tta})_3\text{DPPZ}$, where dbm and tta are statistically localized around the Eu^{3+} . Its observed lifetime, obtained from the monoexponential decay curve, was remarkably shorter than the lifetimes of both individual complexes due to a decrease in the symmetry of the coordination environment of the central ion. Despite this, their PLQYs were equal to those of $\text{Eu}(\text{dbm})_3\text{DPPZ}$ and $\text{Eu}(\text{tta})_3\text{DPPZ}$ (4.8–5.3%).

As a result, the luminance of both MLC-based OLEDs exceeded the luminance of each of the OLEDs based on individual complexes, which confirms the promise of the proposed approach. Although the lifetimes only slightly change in the doped films, even such a slight difference results in the increase of the OLED luminance in the whole bias range. The luminance of the OLEDs, based on the individual complexes, also correlates with the lifetimes, stressing the importance of this parameter.

We suggest that this approach is important as it offers a very simple way to further increase the lanthanide-based OLED efficiency by simply mixing two efficient emitters.

Author contributions

M. I. K.: conceptualization, data curation, investigation, writing – original draft; A. A. V.: investigation, methodology; A. A. P.: investigation, methodology; A. E. A.: investigation; A. S. G.: investigation; E. V. L.: investigation; N. P. K.: methodology, supervision; V. V. U.: conceptualization, formal analysis, funding acquisition, methodology, supervision, writing – review & editing.

Conflicts of interest

There are no conflicts to declare.

Acknowledgements

This work was supported by Russian Science Foundation (RSF 20–73–10053). X-ray diffraction data were performed with the financial support from the Ministry of Science and Higher Education of the Russian Federation using the equipment of Center for molecular composition studies of A.N. Nesmeyanov

Table 2 Electroluminescent properties of the obtained OLEDs based on europium complexes

Complex	OLED number	U_{on} , V	L_{max} , cd m^{-2}
$\text{Eu}(\text{dbm})_3\text{DPPZ}$	1	4.0	381
$\text{Eu}(\text{tta})_3\text{DPPZ}$	2	4.0	255
$\text{Eu}(\text{dbm} + \text{tta})_3\text{DPPZ}$	3	4.0	423
$[\text{Eu}(\text{dbm})_3\text{DPPZ} + \text{Eu}(\text{tta})_3\text{DPPZ}]$	4	4.0	502

Institute of Organoelement Compounds is also gratefully acknowledged.

Notes and references

- 1 T. Tsujimura, *OLED Display Fundamentals and Applications*, John Wiley & Sons, Inc., 2017.
- 2 N. Thejo Kalyani and S. J. Dhoble, *Renewable Sustainable Energy Rev.*, 2015, **44**, 319–347.
- 3 S. O. Jung, Q. Zhao, J.-W. Park, S. O. Kim, Y.-H. Kim, H.-Y. Oh, J. Kim, S.-K. Kwon and Y. Kang, *Org. Electron.*, 2009, **10**, 1066–1073.
- 4 G. Li, T. Fleetham, E. Turner, X.-C. Hang and J. Li, *Adv. Opt. Mater.*, 2015, **3**, 390–397.
- 5 L. G. NanoCell, <https://www.lg.com/uk/lgnanocell/color.jsp>.
- 6 V. V. Utochnikova, in *Handbook on the Physics and Chemistry of Rare Earths*, ed. J.-C. G. Bünzli and V. Pecharsky, Elsevier B. V., 2021.
- 7 J.-C. G. Bünzli and S. V. Eliseeva, *Springer Ser. Fluoresc.*, 2011, **10**, 1–45.
- 8 S. V. Eliseeva and J.-C. G. Bünzli, *Chem. Soc. Rev.*, 2010, **39**, 189–227.
- 9 Y. Chi, T. K. Chang, P. Ganesan and P. Rajakannu, *Coord. Chem. Rev.*, 2017, **346**, 91–100.
- 10 M. L. P. Reddy and K. S. Bejoymohandas, *J. Photochem. Photobiol., C*, 2016, **29**, 29–47.
- 11 J. Jayabharathi, K. Jayamoorthy and V. Thanikachalam, *J. Organomet. Chem.*, 2014, **761**, 74–83.
- 12 H. Uoyama, K. Goushi, K. Shizu, H. Nomura and C. Adachi, *Nature*, 2012, **492**, 234–238.
- 13 Y. Li, J. Y. Liu, Y. Di Zhao and Y. C. Cao, *Mater. Today*, 2017, **20**, 258–266.
- 14 Z. Liu, J. Qiu, F. Wei, J. Wang, X. Liu, M. G. Helander, S. Rodney, Z. Wang, Z. Bian, Z. Lu, M. E. Thompson and C. Huang, *Chem. Mater.*, 2014, **26**, 2368–2373.
- 15 V. V. Utochnikova, A. N. Aslandukov, A. A. Vashchenko, A. S. Goloveshkin, A. A. Alexandrov, R. Grzibovskis and J.-C. G. Bünzli, *Dalton Trans.*, 2021, **50**, 12806–12813.
- 16 J.-C. G. Bünzli and S. V. Eliseeva, *Springer Ser. Fluoresc.*, 2011, **10**, 1–45.
- 17 K. M. Kuznetsov, M. I. Kozlov, A. N. Aslandukov, A. A. Vashchenko, A. V. Medved'ko, E. V. Latipov, A. S. Goloveshkin, D. M. Tsybarenko and V. V. Utochnikova, *Dalton Trans.*, 2021, **50**, 9685–9689.
- 18 M. I. Kozlov, A. N. Aslandukov, A. A. Vashchenko, A. V. Medvedko, A. E. Aleksandrov, E. V. Latipov, A. S. Goloveshkin, D. A. Lypenko, A. R. Tameev and V. V. Utochnikova, *J. Alloys Compd.*, 2021, 161319.
- 19 P. P. Sun, J. P. Duan, H. T. Shih and C. H. Cheng, *Appl. Phys. Lett.*, 2002, **81**, 792–794.
- 20 L. Zhang, B. Li, L. Zhang and Z. Su, *ACS Appl. Mater. Interfaces*, 2009, **1**, 1852–1855.
- 21 H. Xin, F. Y. Li, M. Guan, C. H. Huang, M. Sun, K. Z. Wang, Y. A. Zhang and L. P. Jin, *J. Appl. Phys.*, 2003, **94**, 4729–4731.
- 22 O. Laporte and W. F. Meggers, *J. Opt. Soc. Am.*, 1925, **11**, 459–463.
- 23 K. Binnemans, *Coord. Chem. Rev.*, 2015, **295**, 1–45.
- 24 L. Zhang and B. Li, *J. Lumin.*, 2009, **129**, 1304–1308.
- 25 N. B. D. Lima, S. M. C. Gonçalves, S. A. Júnior and A. M. Simas, *Sci. Rep.*, 2013, **3**, 1–8.
- 26 N. B. D. Lima, J. D. L. Dutra, S. M. C. Gonçalves, R. O. Freire and A. M. Simas, *Sci. Rep.*, 2016, **6**, 21204.
- 27 H. Xu, Q. Sun, Z. An, Y. Wei and X. Liu, *Coord. Chem. Rev.*, 2015, **293–294**, 228–249.
- 28 L. Wang, Z. Zhao, C. Wei, H. Wei, Z. Liu and Z. Bian, *Adv. Opt. Mater.*, 2019, **7**, 1801256.
- 29 J. Kido, K. Nagai, Y. Okamoto and T. Skotheim, *Chem. Lett.*, 1991, 1267–1270.
- 30 J. Kido, H. Hayase, K. Hongawa, K. Nagai and K. Okuyama, *Appl. Phys. Lett.*, 1994, **65**, 2124–2126.
- 31 X.-N. Li, Z.-J. Wu, Z.-J. Si, Z. Liang, X.-J. Liu and H.-J. Zhang, *Phys. Chem. Chem. Phys.*, 2009, **11**, 9687–9695.
- 32 Y. Liu, Y. Wang, J. He, Q. Mei, K. Chen, J. Cui, C. Li, M. Zhu, J. Peng, W. Zhu and Y. Cao, *Org. Electron.*, 2012, **13**, 1038–1043.
- 33 L. R. Melby, N. J. Rose, E. Abramson and J. C. Caris, *J. Am. Chem. Soc.*, 1964, **86**, 5117–5125.
- 34 P. P. Sun, J. P. Duan, J. J. Lih and C. H. Cheng, *Adv. Funct. Mater.*, 2003, **13**, 683–691.
- 35 A. Drozdov and N. Kuzmina, *Comprehensive Inorganic Chemistry II From Elements to Applications*, 2013, pp. 511–534.
- 36 G. Otting, *Annu. Rev. Biophys.*, 2010, **39**, 387–405.
- 37 M. I. Kozlov, A. N. Aslandukov, A. A. Vashchenko, A. Medved'ko, A. E. Aleksandrov, R. Grzibovskis, A. S. Goloveshkin, L. S. Lepnev, A. R. Tameev, A. Vembris and V. V. Utochnikova, *Dalton Trans.*, 2019, **48**, 17298–17309.
- 38 C. Adachi, M. A. Baldo and S. R. Forrest, *J. Appl. Phys.*, 2000, **87**, 8049–8055.
- 39 H. Kanai, S. Ichinosawa and Y. Sato, *Synth. Met.*, 1997, **91**, 195–196.
- 40 M. I. Kozlov, K. M. Kuznetsov, A. S. Goloveshkin, A. Burlakin, M. Sandzhieva, S. V. Makarov, E. Ilina and V. V. Utochnikova, *Materials*, 2023, 16.